The High-temperature Modification of LuAgSn and High-pressure High-temperature Experiments on DyAgSn, HoAgSn, and YbAgSn

Birgit Heying[a], Ute Ch. Rodewald[a], Gunter Heymann[b], Wilfried Hermes[a], Falko M. Schappacher[a], Jan F. Riecken[a], C. Peter Sebastian[c], Hubert Huppertz[b], and Rainer Pöttgen[a]

[a] Institut für Anorganische und Analytische Chemie, Universität Münster, Corrensstraße 30, 48149 Münster, Germany
[b] Department Chemie und Biochemie, Ludwig-Maximilians-Universität München, Butenandtstraße 5 – 13 (Haus D), 81377 München, Germany
[c] Max-Planck-Institut für Chemische Physik fester Stoffe, Nöthnitzer Straße 40, 01187 Dresden, Germany

Reprint requests to R. Pöttgen. E-mail: pottgen@uni-muenster.de

Z. Naturforsch. **2008**, *63b,* 193 – 198; received September 29, 2007

The high-temperature modification of LuAgSn was obtained by arc-melting an equiatomic mixture of the elements followed by quenching the melt on a water-cooled copper crucible. HT-LuAgSn crystallizes with the NdPtSb-type structure, space group $P6_3mc$: a = 463.5(1), c = 723.2(1) pm, $wR2$ = 0.0270, 151 F^2, and 11 variables. The silver and tin atoms build up two-dimensional, puckered $[Ag_3Sn_3]$ networks (276 pm Ag–Sn) that are charge-balanced and separated by the lutetium atoms. The Ag–Sn distances between the $[Ag_3Sn_3]$ layers of 294 pm are much longer. Single crystals of isotypic DyAgSn (a = 468.3(1), c = 734.4(1) pm, $wR2$ = 0.0343, 411 F^2, and 11 variables) and HoAgSn (a = 467.2(1), c = 731.7(2) pm, $wR2$ = 0.0318, 330 F^2, and 11 variables) were obtained from arc-melted samples. Under high-pressure (up to 12.2 GPa) and high-temperature (up to 1470 K) conditions, no transitions to a ZrNiAl-related phase have been observed for DyAgSn, HoAgSn, and YbAgSn. HT-TmAgSn shows Curie-Weiss paramagnetism with μ_{eff} = 7.53(1) μ_B/Tm atom and θ_P = −15.0(5) K. No magnetic ordering was evident down to 3 K. HT-LuAgSn is a Pauli paramagnet. Room-temperature ^{119}Sn Mössbauer spectra of HT-TmAgSn and HT-LuAgSn show singlet resonances with isomer shifts of 1.78(1) and 1.72(1) mm/s, respectively.

Key words: Intermetallics, Stannides, High-pressure Experiments

Introduction

Depending on the size and valence of the rare earth (*RE*) metal, the stannides *RE*AgSn crystallize with five different structure types. With the large trivalent *RE* metals La–Nd, Sm, and Gd–Er they crystallize with the hexagonal NdPtSb-type, while TmAgSn and LuAgSn adopt the ZrNiAl structure. With the smallest rare earth metal scandium the TiFeSi-type occurs, a superstructure of ZrNiAl. In the europium and ytterbium compounds the *RE* elements are divalent. EuAgSn and YbAgSn crystallize with the KHg_2- and YbAgPb-type structures. A literature overview on the crystal chemistry and physical properties of these stannides is given in [1 – 3].

Dimorphism has been observed for ErAgSn and TmAgSn [3]. ErAgSn transforms to a ZrNiAl-type modification under high-pressure (11.5 GPa) high-temperature (1420 K) conditions, and TmAgSn adopts a NdPtSb-type high-temperature modification upon quenching of a sample directly from the melt. We have now extended the high-pressure (HP) high-temperature (HT) experiments to include *RE* = Dy, Ho, and Yb. Herein we report on a new high-temperature modification of LuAgSn, the structure refinements of DyAgSn and HoAgSn, and the magnetic and ^{119}Sn Mössbauer spectroscopic behavior of HT-TmAgSn and HT-LuAgSn.

Experimental Section

Synthesis

Starting materials for the synthesis of the *RE*AgSn samples were rare earth metal ingots (Johnson Matthey), silver wire (Degussa-Hüls, ∅ 1 mm), and tin granules (Merck), all with stated purities better than 99.9 %. For the preparation of HT-LuAgSn, pieces of the lutetium ingot were first arc-melted [4] under argon to a small button (*ca.* 300 mg). The

Table 1. Crystal data and structure refinements for HoAgSn, DyAgSn, and HT-LuAgSn.

Empirical formula	DyAgSn	HoAgSn	HT-LuAgSn
Formula weight, g mol^{-1}	389.06	391.49	401.53
Space group	$P6_3mc$	$P6_3mc$	$P6_3mc$
Unit cell dimensions, pm	a = 468.3(1)	a = 467.2(1)	a = 463.5(1)
(Guinier powder data)	c = 734.4(1)	c = 731.7(2)	c = 723.2(2)
Z	2	2	2
Cell volume, nm^3	V = 0.1395	V = 0.1383	V = 0.1346
Calculated density, gcm^{-3}	9.26	9.40	9.91
Crystal size, μm^3	$20 \times 20 \times 90$	$20 \times 40 \times 40$	$10 \times 20 \times 70$
Transm. ratio (max/min)	1.28	1.88	1.74
Absorption coefficient, mm^{-1}	22.4	23.3	28.0
F(000), e	326	328	336
θ Range for data collection, deg	3 – 32	3 – 32	4 – 32
Range in hkl	± 8, ± 8, ± 13	± 8, ± 8, $-13/+11$	± 8, ± 8, $+11$
Total no. reflections	3642	2821	1274
Independent reflections	411	330	151
$R_{\rm int}$	0.041	0.067	0.062
Reflections with $I \geq 2\sigma(I)$	361	276	132
R_σ	0.017	0.030	0.026
Data / parameters	411 / 11	330 / 11	151 / 11
Goodness-of-fit on F^2	1.072	0.982	1.092
$R1/wR2$ $[I \geq 2\sigma(I)]$	0.016/0.033	0.019/0.029	0.016/0.026
$R1/wR2$ (all data)	0.022/0.034	0.032/0.032	0.022/0.027
BASF	0.43(3)	0.25(5)	0.49(13)
Extinction coefficient	0.0066(8)	0.0035(6)	0.0053(13)
Largest diff. peak/hole, e Å^{-3}	1.52 / −1.42	1.86 / −2.86	1.14 / −1.78

argon was purified with molecular sieves, silica gel, and titanium sponge (900 K). The lutetium button, pieces of the silver wire, and the tin granules were then weighed in the ideal 1 : 1 : 1 atomic ratio and arc-melted under an argon pressure of *ca.* 800 mbar. The button was remelted three times to ensure homogeneity. After the last melting step, the arc was abruptly switched off and the sample was quenched on the water-cooled copper crucible of the arc-melting device. For the transformation to the low-temperature phase, pieces of HT-LuAgSn were sealed in an evacuated silica ampoule and annealed at 970 K for one day. A fresh HT-TmAgSn sample was prepared *via* the same route, and polycrystalline samples of DyAgSn and HoAgSn were obtained directly by arc-melting without further annealing. Due to the high vapour pressure, YbAgSn was prepared in a sealed tantalum tube as described previously [5]. The five *RE*AgSn stannides are stable in air for months.

For the high-pressure high-temperature treatment a multi-anvil assembly was used. For technical details see [6]. Boron nitride crucibles of 14/8-assemblies were loaded with carefully milled DyAgSn, HoAgSn, and YbAgSn, respectively. The assemblies were compressed to 10.5 GPa (12.2 GPa for DyAgSn) and heated to 1470 K (DyAgSn), 1420 K (HoAgSn), and 1370 K (YbAgSn) for 15 min. After holding this temperature for 10 min, the samples were cooled down rapidly (1 min) to 1220 K and annealed for 180 min to enhance the crystallinity. Then, the samples were cooled down to r. t. After the decompression of the assemblies, the recovered octahedral pressure media were broken apart and the samples carefully separated from the surrounding boron nitride crucibles.

X-Ray diffraction

The polycrystalline samples were all characterized through Guinier powder patterns (imaging plate technique, Fujifilm BAS-1800) using Cu$K_{\alpha 1}$ radiation and α-quartz (a = 491.30 and c = 540.46 pm) as an internal standard. The lattice parameters (Table 1) were obtained from least-squares fits of the powder data. The correct indexing of the patterns was ensured through intensity calculations [7] taking the atomic positions from the structure refinements (this work and [3]). The powder and single crystal lattice parameters matched well.

Single crystal intensity data were measured at r. t. by use of a four-circle diffractometer (CAD4) with graphite monochromatized AgK_α radiation (56.086 pm) and a scintillation counter with pulse-height discrimination. The scans were taken in the $\omega/2\theta$ mode and empirical absorption corrections were applied on the basis of ψ-scan data, accompanied by spherical absorption corrections. All relevant details concerning the data collections are listed in Table 1.

Structure refinements

Small, irregularly shaped single crystals of DyAgSn, HoAgSn, and HT-LuAgSn were selected from the crushed

Atom	Wyckoff-position	x	y	z	$U_{11} = U_{22}$	U_{33}	U_{12}	U_{eq}
DyAgSn								
Dy	2*a*	0	0	0[a]	80(1)	72(1)	40(1)	77(1)
Ag	2*b*	2/3	1/3	0.30797(13)	88(3)	148(3)	44(1)	108(2)
Sn	2*b*	2/3	1/3	0.72000(11)	69(2)	89(3)	35(1)	76(1)
HoAgSn								
Ho	2*a*	0	0	0[a]	75(1)	66(2)	37(1)	72(1)
Ag	2*b*	1/3	2/3	0.6907(2)	91(4)	139(6)	46(2)	107(3)
Sn	2*b*	1/3	2/3	0.2803(2)	64(3)	74(5)	32(2)	67(2)
HT-LuAgSn								
Lu	2*a*	0	0	0[a]	79(1)	76(2)	39(1)	78(1)
Ag	2*b*	1/3	2/3	0.6850(5)	91(6)	132(9)	45(3)	105(4)
Sn	2*b*	1/3	2/3	0.2790(6)	77(5)	73(7)	38(2)	76(3)

Table 2. Atomic coordinates and anisotropic displacement parameters (pm^2) for DyAgSn, HoAgSn, HT-LuAgSn. U_{eq} is defined as one third of the trace of the orthogonalized U_{ij} tensor. The anisotropic displacement factor exponent takes the form: $-2\pi^2[(ha^*)^2U_{11} + \ldots + 2hka^*b^*U_{12}]$. $U_{13} = U_{23} = 0$.

[a] Parameter fixed.

Table 3. Interatomic distances (pm), calculated with the lattice parameters taken from X-ray powder data of HT-LuAgSn. All distances within the first coordination spheres are listed. Standard deviations are equal or less than 0.3 pm.

Lu:	3	Ag	299.2	Ag:	3	Sn	276.1	Sn:	3	Ag	276.1
	3	Sn	311.7		1	Sn	293.7		1	Ag	293.7
	3	Sn	335.1		3	Lu	299.2		3	Lu	311.7
	3	Ag	351.4		3	Lu	351.4		3	Lu	335.1
	2	Lu	361.6								

quenched samples and examined by use of a Buerger camera equipped with an image plate system (Fujifilm BAS-1800) in order to establish suitability for intensity data collection. The isotypy with HT-TmAgSn [3] (hexagonal NdPtSb-type [8], space group $P6_3mc$) was already evident from the powder pattern.

The atomic parameters of HT-TmAgSn [3] were taken as starting values and the structures were refined with full-matrix least-squares methods on F^2 using SHELXL-97 [9]. Anisotropic atomic displacement parameters were refined for all atoms. As a check for the correct silver-tin site assignment, the occupancy parameters were refined in separate series of least-squares cycles. All sites were fully occupied within 2 – 3 standard deviations (100.0(6) % Ag and 101.0(7) % Sn for DyAgSn, 97.8(10) % Ag and 100.5(8) % Sn for HoAgSn, 101.3(18) % Ag and 98.8(14) % Sn for HT-LuAgSn), and in the final cycles the ideal occupancy parameters were assumed again. Refinement of the correct absolute structure was ensured through calculation of the Flack parameters [10, 11]. All crystals showed twinning by inversion. The final difference Fourier syntheses were flat (Table 1). The positional parameters and interatomic distances of the refinements are listed in Tables 2 and 3.

Further details of the crystal structure investigation may be obtained from Fachinformationszentrum Karlsruhe, 76344 Eggenstein-Leopoldshafen, Germany (fax: +49-7247-808-666; e-mail: crysdata@fiz-karlsruhe.de, http://www.fiz-informationsdienste.de/en/DB/icsd/depot_anforderung.html) on quoting the deposition number No's. CSD-418582 (DyAgSn), CSD-418581 (HoAgSn), and CSD-418580 (HT-LuAgSn).

EDX analyses

The three single crystals investigated on the diffractometer were studied by energy dispersive analyses of X-rays (EDX) using a Leica 420i scanning electron microscope with the rare earth trifluorides, silver, and tin as standards. The experimentally observed compositions were all close to the ideal ones, and no impurity elements were observed.

Magnetic susceptibility and ^{119}Sn Mössbauer spectroscopy

The HT-TmAgSn and HT-LuAgSn samples were packed in kapton foil and attached to the sample holder rod of a VSM for measuring the magnetic properties in a Quantum Design Physical-Property-Measurement-System in the temperature range 3 – 305 K with magnetic flux densities up to 80 kOe.

A $Ca^{119m}SnO_3$ source was available for the ^{119}Sn Mössbauer spectroscopic investigations. The samples were placed within thin-walled PVC containers at a thickness of about 10 mg Sn/cm^2. A palladium foil of 0.05 mm thickness was used to reduce the tin K X-rays concurrently emitted by this source. The measurements were conducted in the usual transmission geometry at r. t.

Discussion

Crystal chemistry

A new high-temperature modification of LuAgSn has been obtained by quenching the sample from the melt. HT-LuAgSn crystallizes with the NdPtSb-type structure with two formula units per cell. As expected, the cell volume per formula unit of 67.3 Å^3 is slightly higher for HT-LuAgSn as compared to the low-temperature modification (66.9 Å^3) [1]. The structures of DyAgSn and HoAgSn have also been refined

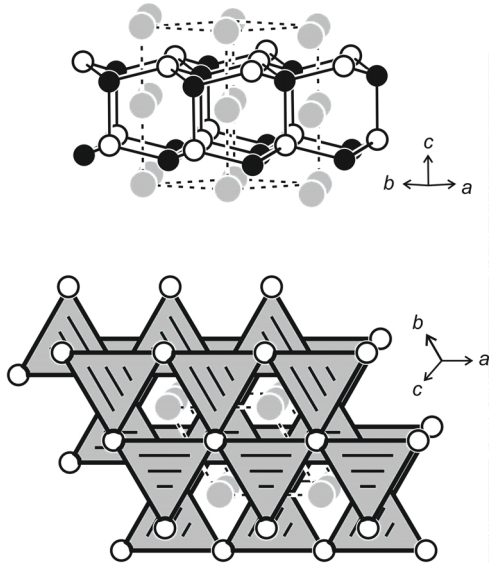

Fig. 1. The crystal structure of HT-LuAgSn. The lutetium, silver, and tin atoms are drawn as medium grey, black, and open circles, respectively. The network of puckered Ag_3Sn_3 hexagons is emphasized at the top while the bottom drawing emphasizes the network of corner-sharing $AgSn_{4/4}$ tetrahedra.

from single crystal diffractometer data. Neutron powder diffraction data of both stannides were published by Baran *et al.* [12]. The resolution of the reported patterns was poor, and the silver and tin sites were mixed up, leading to a wrong assignment of the coordination of the rare earth atoms. Herein, we report precise single crystal data, which undoubtedly revealed the correct silver and tin sites with much higher precision than the neutron data. The refined occupancy parameters (*vide supra*) gave no hint for silver-tin mixing.

As an example, we briefly discuss the HT-LuAgSn structure. Each silver atom has four tin neighbors in an elongated tetrahedral coordination (3×276 and 1×294 pm Ag–Sn). The shorter Ag–Sn distances compare well with the sum of the covalent radii of 274 pm [13]. Within the *ab* plane (Fig. 1) the Ag–Sn distances are short, but longer between these layers. The $AgSn_{4/4}$ tetrahedra are condensed *via* all corners leading to a three-dimensional wurtzite-related network in which the lutetium atoms fill cages. The bonding of the lutetium atoms to the [AgSn] network proceeds *via* shorter Lu–Ag distances of 299 pm, only slightly longer than the sum of the covalent radii of 290 pm [13]. In the wrong structural model, proposed by Baran *et al*. [12], the lutetium atoms would have nearest tin neighbors. The structural model of the *RE*AgSn stannides reported herein is in perfect agreement with the recently reported stannides *RE*AuSn (*RE* = Sm, Gd, Tm) [14], where the gold and tin atoms have significantly different scattering power.

The NdPtSb-type *RE*AgSn stannides are superstructures of the AlB_2-type. For further details on the crystal chemistry and chemical bonding in this family of compounds we refer to recent review articles [15 – 17].

Magnetism and ^{119}Sn Mössbauer spectroscopy

The temperature dependence of the magnetic susceptibility of HT-TmAgSn and HT-LuAgSn is presented in Fig. 2. HT-LuAgSn with diamagnetic lutetium(III) is Pauli paramagnetic with an almost temperature independent negative susceptibility of $-9.8(2) \times 10^{-5}$ emu/mol at r. t. The strong intrinsic diamagnetic contribution overcompensates the weak Pauli contribution, leading to negative susceptibility values. The small increase at low temperature is due to trace amounts of paramagnetic impurities.

HT-TmAgSn shows Curie-Weiss behavior. Evaluation of the temperature range 100 – 300 K gave an experimental magnetic moment of 7.53(1) μ_B/Tm atom and a Weiss constant $\theta_P = -15.0(5)$ K, indicating antiferromagnetic interactions. The experimental moment is close to the free ion value of 7.56 μ_B for Tm^{3+}. No hint for magnetic ordering was evident down to the lowest available temperature of 3 K, similar to LT-TmAgSn [1]. The magnetization as a function of

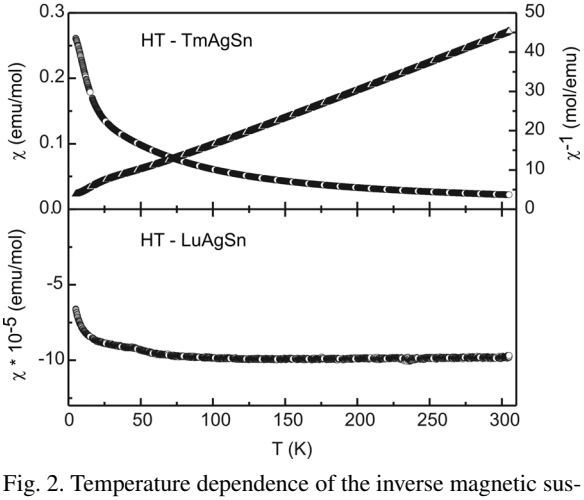

Fig. 2. Temperature dependence of the inverse magnetic susceptibility of HT-TmAgSn and the magnetic susceptibility of HT-LuAgSn measured at 10 kOe.

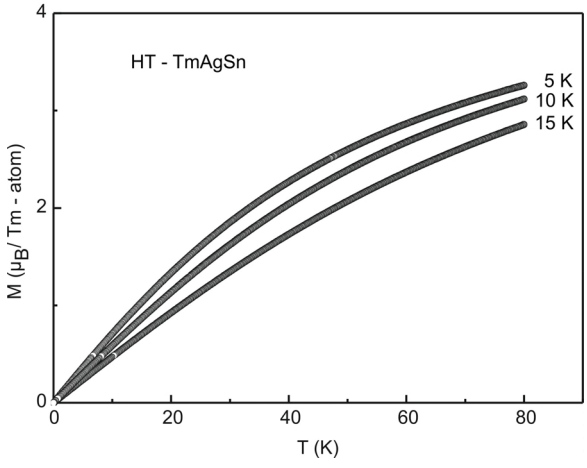

Fig. 3. Magnetization *vs.* external magnetic field for HT-TmAgSn at 5, 10, and 15 K.

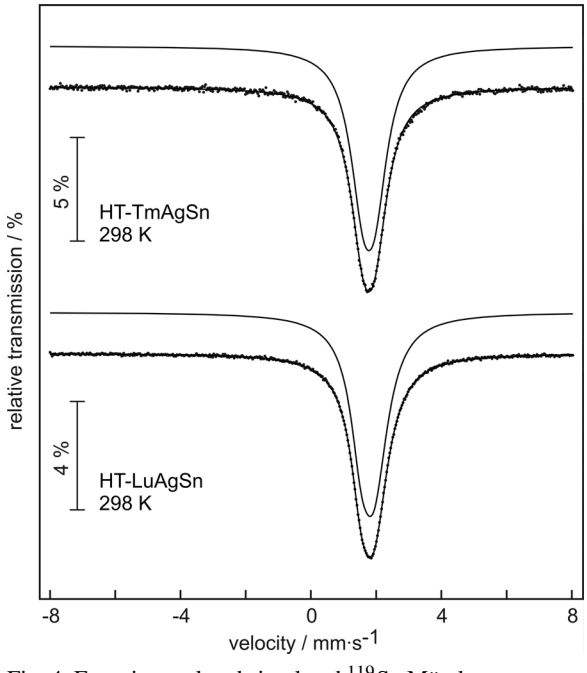

Fig. 4. Experimental and simulated ^{119}Sn Mössbauer spectra of HT-TmAgSn and HT-LuAgSn.

the external field (Fig. 3) increases in a curvilinear fashion at 15 K, while a slightly stronger curvature is observed at 5 K. The magnetization at 80 kOe and 5 K is 3.26(1) μ_B/Tm atom, much smaller than the theoretical saturation magnetization value of 7.0 μ_B for Tm^{3+}.

The ^{119}Sn Mössbauer spectra of HT-TmAgSn and HT-LuAgSn at r.t. are shown in Fig. 4 together with transmission integral fits. Both stannides show singlet resonances in agreement with the crystallographic results. The fitting parameters are δ = 1.78(1) mm/s, ΔE_Q = 0.38(1) mm/s, Γ = 0.96(1) mm/s for HT-TmAgSn and δ = 1.72(1) mm/s, ΔE_Q = 0.40(1) mm/s, Γ = 0.72(2) mm/s for HT-LuAgSn. The slightly higher line width of the HT-TmAgSn sample with respect to HT-LuAgSn might be indicative of some disorder within the polycrystalline sample. Similar to the low-temperature modifications, HT-LuAgSn also reveals a smaller isomer shift than HT-TmAgSn. This reflects the course of the electronegativities in the *RE*AgSn series. The less electronegative lutetium atoms (when compared with thulium) transfer less electron density to the [AgSn] network, and consequently we observe a smaller electron density at the tin nuclei. Similar behavior has been observed in the *RE*CuSn [18, 19] and *RE*AuSn [20] series.

High-pressure high-temperature experiments on DyAgSn, HoAgSn, and YbAgSn

In continuation of the high-pressure high-temperature experiments on ErAgSn [3], we have tested the HP-HT behavior of the neighboring stannides DyAgSn, HoAgSn, and YbAgSn. The ytterbium compound was treated under 10.5 GPa at 1370 K. The X-ray powder pattern gave no hint for a structural transition. The decompressed sample corresponds to the initial one. The refined lattice parameters (a = 479.3(2), c = 1089.3(4) pm) compared well to the original ones for YbAgPb-type YbAgSn [5].

In contrast to these results, we observed decomposition of the DyAgSn and HoAgSn samples under high-pressure (12.2 GPa for DyAgSn and 10.5 GPa for HoAgSn) high-temperature (1470 K for DyAgSn and 1420 K for HoAgSn) conditions. The HP-HT treated DyAgSn contained residual DyAgSn with NdPtSb structure (a = 466.3, c = 736.6 pm), Cu_3Au-type $Dy(Ag/Sn)_3$ (a = 453.8 pm) as the main phase, and a trace of orthorhombic $Dy_3Ag_4Sn_4$ [21]. The lattice parameter for the cubic phase is close to that of the recently reported phase $Dy(Ag_{1/3}Sn_{2/3})_3$ (a = 453.1 pm) [21], and we can assume a similar composition for our multiphase sample.

The main phase of the HoAgSn sample was unreacted equiatomic HoAgSn (a = 467.5(2), c = 732.4(2) pm) besides $Ho(Ag_{1/3}Sn_{2/3})_3$ (a = 449.3 pm) and a trace amount of $Ho_3Ag_4Sn_4$. Since the reflec-

tions for both $RE_3Ag_4Sn_4$ phases were very weak, reliable refinement of the lattice parameters was not possible.

Summing up, ytterbium remains in a stable divalent state in YbAgSn also under the applied HP-HT conditions and does not transform to a ZrNiAl-type phase. In DyAgSn and HoAgSn, the rare earth atoms most likely are too large to allow any dimorphism as observed for ErAgSn [3].

Acknowledgements

This work was financially supported by the Deutsche Forschungsgemeinschaft (Po573/10-1 and HU966/4-1) and the European Science Foundation through the COST D30/003/03 network *Development of Materials Chemistry using High-Pressures*. We thank Prof. Dr. W. Schnick (LMU München) for the continuous support of these investigations. H. Huppertz is indebted to the Fonds der Chemischen Industrie for financial support.

[1] C. P. Sebastian, H. Eckert, C. Fehse, J. P. Wright, J. P. Attfield, D. Johrendt, S. Rayaprol, R.-D. Hoffmann, R. Pöttgen, *J. Solid State Chem.* **2006**, *179*, 2376.
[2] C. P. Sebastian, L. Zhang, H. Eckert, C. Fehse, R.-D. Hoffmann, R. Pöttgen, *Inorg. Chem.* **2007**, *46*, 711.
[3] C. P. Sebastian, G. Heymann, B. Heying, U. Ch. Rodewald, H. Huppertz, R. Pöttgen, *Z. Anorg. Allg. Chem.* **2007**, *633*, 1551.
[4] R. Pöttgen, Th. Gulden, A. Simon, *GIT Labor-Fachzeitschrift* **1999**, *43*, 133.
[5] R. Pöttgen, P. Arpe, C. Felser, D. Kußmann, R. Müllmann, B. D. Mosel, B. Künnen, G. Kotzyba, *J. Solid State Chem.* **1999**, *145*, 668.
[6] H. Huppertz, *Z. Kristallogr.* **2004**, *219*, 330.
[7] K. Yvon, W. Jeitschko, E. Parthé, *J. Appl. Crystallogr.* **1977**, *10*, 73.
[8] G. Wenski, A. Mewis, *Z. Kristallogr.* **1986**, *176*, 125.
[9] G. M. Sheldrick, SHELXL-97, Program for Crystal Structure Refinement, University of Göttingen, Göttingen (Germany) **1997**.
[10] H. D. Flack, G. Bernadinelli, *Acta Crystallogr. A*, **1999**, *55*, 908.
[11] H. D. Flack, G. Bernadinelli, *J. Appl. Crystallogr.* **2000**, *33*, 1143.
[12] S. Baran, J. Leciejewicz, N. Stüsser, A. Szytuła, A. Zygmunt, Y. Ding, *J. Magn. Magn. Mater.* **1997**, *170*, 143.
[13] J. Emsley, *The Elements*, Oxford University Press, Oxford, **1999**.
[14] C. P. Sebastian, R. Pöttgen, *Z. Naturforsch.* **2006**, *61b*, 1045.
[15] R.-D. Hoffmann, R. Pöttgen, *Z. Kristallogr.* **2001**, *216*, 127.
[16] M. D. Bojin, R. Hoffmann, *Helv. Chim. Acta* **2003**, *86*, 1653.
[17] M. D. Bojin, R. Hoffmann, *Helv. Chim. Acta* **2003**, *86*, 1683.
[18] C. P. Sebastian, C. Fehse, H. Eckert, R.-D. Hoffmann, R. Pöttgen, *Solid State Sci.* **2006**, *8*, 1386.
[19] C. P. Sebastian, S. Rayaprol, R. Pöttgen, *Solid State Commun.* **2006**, *140*, 276.
[20] C. P. Sebastian, H. Eckert, S. Rayaprol, R.-D. Hoffmann, R. Pöttgen, *Solid State Sci.* **2006**, *8*, 560.
[21] V. V. Romaka, A. Tkachuk, V. Davydov, *J. Alloys Compd.* **2007**, *439*, 128.